Arabinosylcytosine Stability in Aqueous Solutions: pH Profile and Shelflife Predictions

ROBERT E. NOTARI▲, MARILYN LUE CHIN, and RICHARD WITTEBORT*

Abstract □ Apparent first-order rate constants, k, for the degradation of arabinosylcytosine in aqueous solutions were determined as a function of pH, temperature, and buffer concentrations. Profiles showing the effect of pH on k were constructed from data obtained in hydrochloric acid and sodium hydroxide and by extrapolation of buffer data to zero buffer concentration. Maximum stability is observed in the neutral pH region where arabinosylcytosine undergoes deamination to arabinosyluracil and 90% potency is maintained for 6.5 months in 0.06 M phosphate buffer, pH 6.9, at 25°. The observed rate constant, k, increases as the pH decreases from 6 to 2.8, where it passes through a maximum value and again decreases as the pH approaches zero. In the pH region 0–6, the loss of substrate is accompanied by the formation of an intermediate which reacts further to yield arabinosyluracil. The profile for the maximum yields of the intermediate as a function of pH resembles the k *versus* pH profile. Kinetics for deuterium exchange at the H_5 on arabinosylcytosine and TLC studies characterizing the intermediate were combined with the other kinetic data in developing a proposed mechanism involving 2′-hydroxyl participation and the formation of an intermediate in acid pH. In alkaline solutions the loss of arabinosylcytosine is about 10 times more rapid than in acid and most likely is due to hydrolysis of the pyrimidine ring since no arabinosyluracil UV absorption spectra were detected.

Keyphrases □ Arabinosylcytosine stability in aqueous solutions—pH profile, shelflife predictions □ pH profile—arabinosylcytosine stability in aqueous solutions

Arabinosylcytosine[1], I, has been clinically proven to be a markedly effective antileukemic agent and is now marketed[2] as such. It is a synthetic analog of naturally occurring arabinosyluracil, II, which has been extracted from certain sponges found only in the Caribbean (1). In general, few cases of solid tumors have benefited from I but remissions have occurred in substantial numbers of children and adults with acute leukemia (2, 3). The greatest beneficial response appears to be in acute granulocytic leukemia, for which I has shown a 24% remission rate.

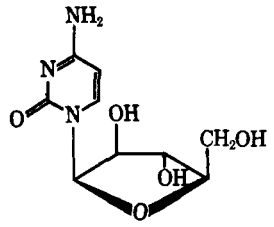

I

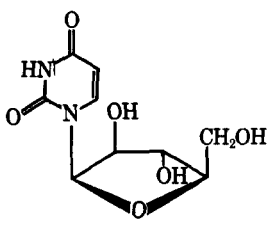

II

Arabinosylcytosine is clinically available as a freeze-dried preparation[2] to be reconstituted for injection at the time of use. In aqueous buffered solutions, I has been shown to undergo hydrolytic deamination to form the inactive nucleoside, II (4). The stability of I in aqueous solution is, therefore, of pharmaceutical interest with regard to storage or admixture with other agents. This paper provides data for the stability of I as a function of pH in aqueous solutions at 70 and 80° together with the necessary parameters for calculating shelflife at other temperatures. The catalytic effects of a number of buffers were evaluated, and a prediction of the shelflife at room temperature under conditions for maximum stability is included.

EXPERIMENTAL

Kinetics of Arabinosylcytosine Loss—Reaction solutions containing I in the presence of excess hydrochloric acid, buffer, or sodium hydroxide were prepared as shown in Tables I–III. All long-term studies were conducted in sealed ampuls. Short-term reactions ($t_{1/2}$ < 15 hr.) were carried out in glass-stoppered flasks. Reactions in the pH range 0–5 (Tables I and II) were assayed as a function of time by determining the absorbance at 260 and 280 nm. after diluting an aliquot with an appropriate volume of 0.1 M HCl and solving for the concentrations from Eqs. 1 and 2, which have been shown to be applicable to mixtures of I and II (4):

$$\mathrm{I} = (0.928A_{280} - 0.389A_{260}) \times 10^{-4} \quad \text{(Eq. 1)}$$

$$\mathrm{II} = (1.21A_{260} - 0.541A_{280}) \times 10^{-4} \quad \text{(Eq. 2)}$$

Table I—Experimental Conditions and Apparent First-Order Rate Constants for Arabinosylcytosine[a] Loss in Hydrochloric Acid

70°				80°			
10 [HCl]	10^2k, hr.$^{-1}$	10 [HCl]	10^2k, hr.$^{-1}$	10 [HCl]	10^2k, hr.$^{-1}$	10 [HCl]	10^2k, hr.$^{-1}$
9.56	1.95	1.91	2.62	9.56	4.46	1.91	5.78
7.64	1.95	0.458	2.91	7.64	4.76	0.458	6.96
5.73	2.14	0.092	3.29	5.73	5.06	0.092	7.50
3.82	2.38	—	—	3.82	5.39	—	—

[a] Initial concentrations: 5×10^{-5} M, 80°; 5×10^{-4} M, 70°. The 80° reactions were assayed without dilution.

[1] There are several names for this nucleoside in the literature. The chemical name is 1β-D-arabinofuranosylcytosine; the USAN name is cytarabine; the IUPAC name is arabinosylcytosine; and the common (though incorrect) name is cytosine arabinoside. The approved abbreviation is Ara-C (also incorrectly abbreviated CA).

[2] Cytosar, Upjohn.

Table II—Experimental Conditions and Apparent First-Order Rate Constants for Loss of 5×10^{-4} *M* Arabinosylcytosine in the Presence of Buffers in the pH Region 2.8–4.5

Temperature	pH	Buffer [HCO_2H]	Buffer [HCO_2Na]	Buffer [NaCl]	10^3k, $hr.^{-1}$
70°	2.87 ±0.08	0.35	0.035	0.31	59.8
		0.25	0.025	0.32	58.1
		0.15	0.015	0.33	55.6
		0.10	0.010	0.34	52.1
		0.05	0.005	0.34	47.0
70°	3.15 ±0.05	0.105	0.035	0.31	56.4
		0.075	0.025	0.32	55.0
		0.045	0.015	0.33	51.5
		0.030	0.010	0.34	47.0
		0.015	0.005	0.34	40.8
70°	3.61 ±0.08	0.35	0.35	0.00	73.8
		0.30	0.30	0.05	70.2
		0.25	0.25	0.10	67.6
		0.20	0.20	0.15	62.8
		0.10	0.10	0.25	55.9
		0.035	0.035	0.31	46.5
		0.025	0.025	0.32	43.8
		0.015	0.015	0.33	40.1
		0.010	0.010	0.34	35.9
		0.005	0.005	0.34	30.7
70°	3.90 ±0.05	0.020	0.040	0.31	35.1
		0.015	0.030	0.32	33.2
		0.010	0.020	0.33	30.8
		0.008	0.016	0.33	29.1
		0.003	0.006	0.34	22.4
70°	4.18 ±0.03	0.010	0.040	0.31	24.4
		0.008	0.032	0.32	22.9
		0.006	0.024	0.33	21.1
		0.004	0.016	0.33	18.8
		0.002	0.008	0.34	16.3
70°	4.49 ±0.04	0.035	0.35	0.00	26.7
		0.030	0.30	0.05	25.8
		0.025	0.25	0.10	24.4
		0.020	0.20	0.15	22.4
		0.010	0.10	0.25	17.9
80°	3.50 ±0.06	0.390	0.352	0.00	165
		0.338	0.304	0.05	159
		0.222	0.200	0.15	137
		0.106	0.096	0.26	119
		0.018	0.016	0.34	81.8
		0.009	0.008	0.35	72.4
		0.004	0.004	0.35	61.5
		[CH_3-CHO-HCO_2H]	[CH_3CHO-HCO_2Na]	[NaCl]	
80°	2.79 ±0.05	2.95	0.35	0.00	155
		1.71	0.20	0.15	153
		0.86	0.10	0.25	138
		0.086	0.01	0.34	103
80°	4.05 ±0.03	0.259	0.35	0.00	113
		0.148	0.20	0.15	102
		0.072	0.10	0.25	81.3
		0.007	0.01	0.34	52.3
80°	4.18 ±0.04	0.107	0.352	0.00	77.5
		0.061	0.200	0.15	62.4
		0.024	0.080	0.27	52.9
		0.002	0.008	0.34	31.3

In the alkaline pH region (Table III), the loss of I was not accompanied by a corresponding increase in the concentration of II. Instead, the UV absorption spectrum of I was found to decrease as a function of time without the appearance of any new spectra. Therefore, the alkaline kinetic runs were carried out by diluting reaction aliquots with 0.1 *M* HCl and determining the UV absorbance spectra as a function of time. Absorbance data were then used directly to calculate the apparent first-order rate constants.

Kinetics of Deuterium Exchange and Deamination in Deuterated Solvents—Exchanging deuterium for the H_5 proton of cytosine nucleosides results in the collapse of the H_6 proton doublet to a singlet (Fig. 1). Santi *et al.* (5) showed that the percent deuterium exchange at H_5 is linearly related to the fraction, *f*, where:

$$f = (A + B)/(A + B + C) \qquad \text{(Eq. 3)}$$

Table III—Experimental Conditions and Apparent First-Order Rate Constants Determined from the Decrease in UV Absorbance Due to Loss of 6×10^{-4} *M* Arabinosylcytosine in Alkaline pH

pH	Buffer	10^3k, $hr.^{-1}$
	70°	
8.92[a]	0.02 Borate[a]	0.739
8.92	0.01 Borate	0.709
8.92	0.005 Borate	0.655
8.92	(Unbuffered)	0.575[c]
10.78[b]	0.01 NaOH	8.23
11.28[b]	0.04 NaOH	36.8
11.63[b]	0.10 NaOH	66.9
12.58[b]	1.00 NaOH	315
	80°	
11.00[b]	0.04 NaOH	77.3
11.43[b]	0.10 NaOH	168
12.35[b]	1.00 NaOH	792

[a] Taken from "Documenta Geigy Scientific Tables," 7th ed., p. 279. [b] Calculated using literature values for activity coefficients (10), except for 0.01 *N* where the value $\gamma = 1$ was used. [c] Extrapolated from buffer data.

and *A* and *B* are the peak heights of the doublet and *C* is the peak height of the singlet as shown in Fig. 1. This linear relationship is independent of the "R" group at N-1 (5). However, the slope of the line, *f versus* % D, may vary with R. To determine the exact % D, it is necessary to construct a calibration plot. Since the parameter *f* is linearly related to % D, the values of *f* can be used directly to calculate first-order rate constants for exchange. It is, therefore, unnecessary to know the absolute values of % D to obtain the rate constants.

Monodeuteroacetic acid, deuterium chloride, deutero sodium hydroxide, and deuterium oxide[3] were used to prepare the buffers listed in Table IV. The ionic strength was adjusted to 0.36 with sodium chloride. The pD values of the buffer solutions were determined by adding 0.4 to the pH readings of the deuterium oxide solutions at 70° (6). The readings were determined with a microelectrode (pH 0–14, 0–80°), and a digital-reading pH meter[4] which was calibrated with two standard buffers. The reaction mixture was injected into an NMR tube which was then placed in a 70° constant-temperature bath. At various intervals, the tube was withdrawn and the NMR spectrum from 450 to 500 Hz. was determined[5]. Spectrophotometric assays for I and II in the mixtures were performed in triplicate as a function of time by diluting 3 μl. of the reaction mixture with 25 ml. of 0.1 *M* HCl and determining the absorbance at 260 and 280 nm. Equations 1 and 2 were then employed for I and II concentrations.

Effects of Reaction Conditions on Intermediate Formation—Material balance was monitored during all studies by summing the concentrations of I and II throughout the reaction. The concentration of additional component(s) was calculated from the equation:

$$(X) = (I)_0 - (I + II) \qquad \text{(Eq. 4)}$$

Thus, the concentrations of the reaction components (I, II, and *X*) were calculated for each reaction sample and results were plotted as a function of time. Figure 2 shows a typical time course for the three components. The shape of these plots is characteristic of a series of rate processes where *X* represents an intermediate formed during the hydrolysis of I to II.

UV Absorption Characteristics of *X*—A reaction mixture containing 39.6% I, 41.4% *X*, and 19% II in formic acid–formate (0.0177–0.0016) buffer was assayed with a spectrophotometer[6], and the UV absorption spectrum from 400 to 220 nm. was determined using a spectrophotometer[7]. A simulated mixture containing calculated amounts of I and II was prepared in formic acid–formate (0.0177–0.0016) buffer, and its absorption spectrum from 400 to 220 nm. was determined. The difference between these plots of ab-

[3] E. Merck A. G., Darmstadt, W. Germany.
[4] Sargeant model DR.
[5] Using a Varian A-60A.
[6] Beckman DU.
[7] Cary 15.

Table IV—Experimental Conditions and Apparent First-Order Rate Constants for Deuterium Exchange and Deamination of 0.5 *M* Arabinosylcytosine in Deuterium Oxide at 70°[a]

pD	$[CH_3CO_2D]$	$[CH_3CO_2Na]$	Exchange	Deamination
5.15	0.3	0.03	95	0.97
4.74	1.0	0.10	134	2.24
4.47	2.0	0.20	181	3.08

[a] μ adjusted to 0.36 with sodium chloride.

sorbance as a function of wavelength represents the spectrum for the 41.4% *X* in the original mixture.

The absorption spectrum of *X* was also determined under alkaline conditions as follows. Four milliliters of reaction mixture was diluted to 25 ml. with 0.1 *M* Na_2HPO_4 solution, and the absorption spectrum of the resulting solution was determined from 330 to 220 nm. at various time intervals. First-order plots for the increase in absorbance at various wavelengths due to arabinosyluracil formation were extrapolated to the *Y*-axis to obtain absorbance values at zero time. These values were then compared with the spectrum of a simulated mixture containing the calculated amounts of I and II in 0.1 *M* Na_2HPO_4.

Spectrophotometric Differential Assay for *X*—A UV assay for the concentration of *X* in a reaction mixture was developed. The basis for the assay is the quantitative conversion of *X* to II. Thus, the analysis of II in the reaction mixture before and after complete conversion allows one to calculate the concentration of *X* from:

$$(X) = (\mathrm{II})_f - (\mathrm{II})_i \qquad \text{(Eq. 5)}$$

where $(\mathrm{II})_f$ is the final concentration and $(\mathrm{II})_i$ is the initial concentration. Complete conversion of *X* to II can be achieved within minutes by warming the solutions under mildly alkaline conditions. The following example illustrates the application of this property to the assay of *X* in a reaction mixture.

A reaction mixture containing 0.0005 *M* I in formic acid–formate (0.0177–0.0016) buffer was heated to 70° for 25 hr. The mixture was then assayed by determining the absorbance at 260 and 280 nm. after diluting 2 ml. to 25 ml. with 0.1 *M* HCl and applying Eqs. 1 and 2. A second assay was performed by adding 2 ml. boric acid (0.32 *M*)–borate (0.32 *M*) buffer to 2 ml. of reaction mixture and warming the resulting solution to 35° for 10 min. This solution was then diluted to 25 ml. with 0.1 *M* HCl and assayed in the manner already described.

TLC Separation of Reaction Components—Three types of TLC were employed to separate reaction components: one dimensional, two dimensional, and preparative. The two developing solvents employed in each case were benzene–methanol (3:1) and water-saturated butanol–propanol (3:1). Plates were coated with a 0.25-mm. layer of silica gel GF_{254} slurry in either water or 0.1 *M* HCl except for the preparative scale studies for which a 1-mm. thick slurry in 0.1 *M* HCl was employed.

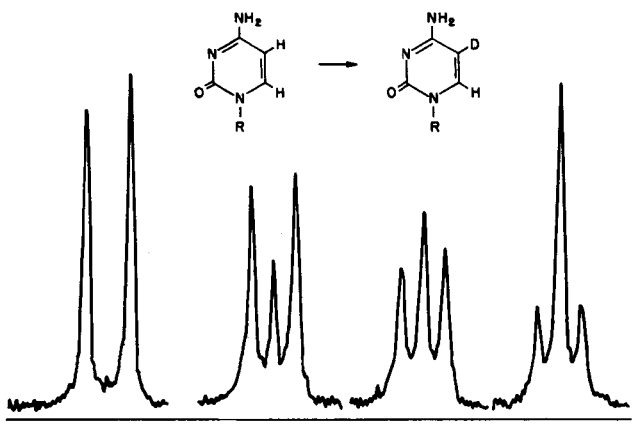

Figure 1—*Change of the 480-Hz. NMR signal for H_6 from a doublet to a singlet during the exchange of the H_5 proton of arabinosylcytosine for deuterium under the conditions in Table IV.*

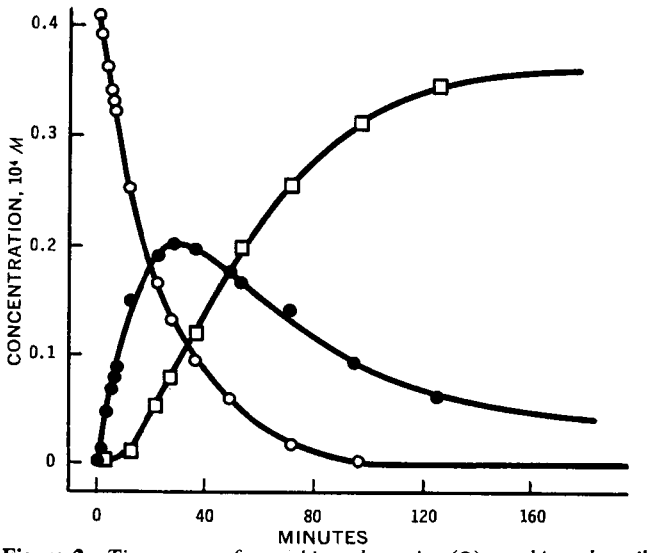

Figure 2—*Time course for arabinosylcytosine* (○), *arabinosyluracil* (□), *and the intermediate*, X (●), *during the deamination of arabinosylcytosine in formate buffer, pH 3.2, 70°.*

One-dimensional chromatography was used routinely to monitor deamination of I by comparing reaction components to reference standards for I and II. Two-dimensional chromatography was employed in the following manner. Compound I (0.05 *M*) was heated in formic acid (0.088 *M*)-formate (0.008 *M*) buffer at 70° for 14 hr. The resultant mixture was chromatographed on a 20 × 20-cm. plate coated with silica gel GF_{254} in 0.1 *M* HCl. After developing, the solvent was allowed to evaporate and the plate was sprayed with 0.1 *M* NaOH and allowed to dry. Then the plate was again developed in the same solvent but in a direction perpendicular to the first.

Preparative scale TLC separation was carried out on a reaction mixture containing 0.032 *M* I in 0.01 *M* HCOOH and 0.033 *M* HCl which was allowed to react at 70° for 36 hr. The reaction was concentrated from 20 to 1.2 ml. with a flash evaporator. Temperatures lower than 35° were employed in the evaporation procedure. The concentrate was then streaked on six 20 × 20-cm. plates so that each plate contained an equal amount of concentrate. A control which contained no reaction mixture was developed together with the streaked plates to a height of 15 cm. with water-saturated butanol–propanol (3:1). After developing and drying, the middle bands (R_f 0.49) from the six plates were eluted with 0.1 *M* HCOOH in three divided portions totaling 16 ml. Each fraction was passed through a sintered-glass filter. The combined filtrate was concentrated to a volume of 1 ml. and assayed for *X*.

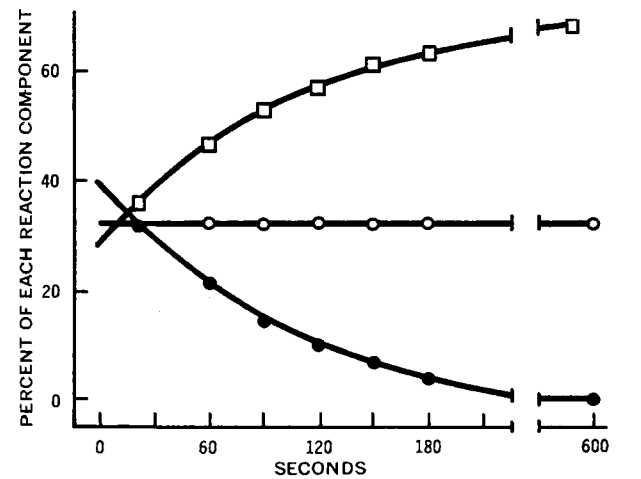

Figure 3—*Change in percentage composition as a function of time of an acidic reaction mixture when placed in borate buffer at 35°, pH 9, where* ○ *is arabinosylcytosine,* □ *is arabinosyluracil, and* ● *is the intermediate*, X.

Table V—Experimental Conditions and Pseudo-First-Order Rate Constants for Conversion of 3.3×10^{-5} *M X* to II in Phosphate and Borate Buffers

Temperature	pH	$[NaH_2PO_4]$	$[Na_2HPO_4]$	[NaCl]	k, hr.$^{-1}$
55.5°	5.55 ± 0.05	0.25	0.025	0.035	2.15
		0.15	0.015	0.165	1.45
		0.08	0.008	0.256	0.75
		0.02	0.002	0.334	0.23
	6.58 ± 0.07	0.09	0.09	0.00	8.17
		0.06	0.06	0.12	5.65
		0.03	0.03	0.24	2.85
		0.01	0.01	0.32	1.20
	7.55 ± 0.07	0.010	0.10	0.050	12.20
		0.008	0.08	0.112	10.55
		0.005	0.05	0.205	7.78
		0.002	0.02	0.298	4.45
45.0°	6.58 ± 0.07	0.081	0.081	0.00	3.81
		0.054	0.054	0.12	2.307
		0.030	0.030	0.24	1.382
		0.010	0.010	0.32	0.473
	7.55 ± 0.07	0.010	0.10	0.050	4.82
		0.008	0.08	0.112	4.76
		0.005	0.05	0.205	3.21
		0.002	0.02	0.298	1.71
		H_3BO_3	$H_2BO_3^-$	NaCl	
	8.97 ± 0.07	0.20	0.20	0.16	46.0
		0.10	0.10	0.26	32.8
		0.05	0.05	0.31	26.0

Kinetics of Instability of the Intermediate X—It is apparent from the previous sections that *X* can best be produced at low pH and low buffer concentrations but that *X* is very unstable in the presence of base. Since I and II are relatively stable at lower temperatures (Fig. 3, for example), the kinetics of loss of *X* were studied by producing *X* in a reaction mixture at high temperature and studying its loss in buffers at low temperatures. The concentration of I remained constant throughout the loss of *X* during all studies, and the final concentration of II after complete conversion of *X* remained constant and equal to $(I)_0 - (I)_t$. An example of a typical procedure follows.

A solution containing 0.0329 *M* I, 0.01 *M* formic acid, and 0.033 *M* HCl (pH 2.7) was allowed to react at 70° for 36 hr., after which approximately 50% of the initial concentration of I was converted to *X*. One milliliter of this reaction mixture was added to 49 ml. of the buffer which was equilibrated to the desired temperature. The reaction was quenched as a function of time by diluting 2-ml. aliquots with 25 ml. of 0.1 *M* HCl, and the dilutions were assayed for I and II by Eqs. 1 and 2. The concentration of *X* as a function of time was calculated according to Eq. 4, and first-order plots were constructed. Experimental conditions are listed in Table V. The

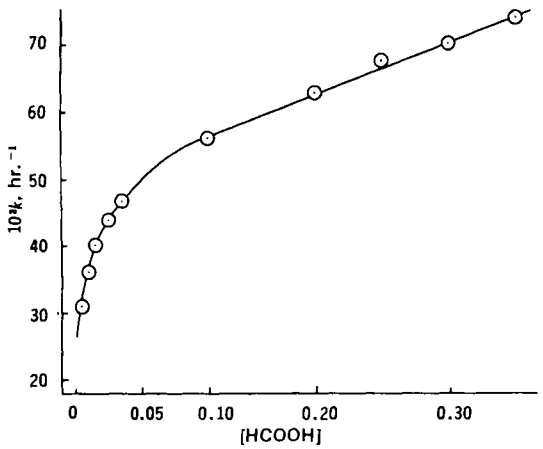

Figure 4—*Apparent first-order rate constants for loss of arabinosylcytosine in formate buffer, pH 3.6, 70°, as a function of formic acid concentration.*

Table VI—Apparent First-Order Rate Constants, k in hr.$^{-1}$, for Loss of Arabinosylcytosine as a Function of pH[a]

Buffer	pH	10^3k
	70°	
Hydrochloric acid[b]	0.15	19.5
	0.26	19.5
	0.38	21.4
	0.56	23.8
	0.86	26.2
	1.42	29.1
	2.08	32.9
Formate	2.87	37
	3.15	35
	3.61	26[c]
Acetate[d]	3.66	34
Formate	3.90	18
	4.18	13
	4.49	12
Acetate[d]	4.71	10
	5.66	1.4
Phosphate[e]	6.15	0.71
	6.90	0.29
	7.81	0.38
	80°	
Hydrochloric acid[b]	0.16	44.6
	0.27	47.6
	0.39	50.6
	0.56	53.9
	0.85	57.8
	1.43	69.6
	2.08	75.0
Lactate	2.79	96[f]
Formate	3.50	47
Acetate[d]	3.66	90
Lactate	4.05	48
	4.18	28
Acetate[d]	4.72	18
	5.66	3.5

[a] Rate constants in pH region 2.8–5.7 were determined by obtaining the intercepts of k_1 *versus* buffer concentration using a polynomial regression on an IBM 360/75, where the degree of the polynomial was chosen so that the percent error between the resultant curve and the data had the limits $0 <$ (percent error) < 3. Intercepts in phosphate buffers were determined from linear plots of k_1 *versus* buffer concentration. [b] The pH of hydrochloric acid solutions was calculated using literature values for activity coefficients (11). [c] This value was used for the pH profile since the formate series at pH 3.61 includes more dilute buffers than the acetate system (Fig. 4). [d] Taken from *Reference 4*. [e] Taken from *Reference 7*. [f] This value agrees with the observed constant in dilute formate at pH 2.8 (HCO_2H = 0.02, HCO_2Na = 0.002), which is 97×10^{-3} (hr.$^{-1}$).

effect of the formate ion is negligible since its concentration is 2×10^{-4} *M*.

RESULTS

Kinetics of Arabinosylcytosine Loss—The concentrations of I, II, and *X* were determined as a function of time in the neutral and acid pH region using Eqs. 1, 2, and 4. Pseudo-first-order rate constants for the loss of I were calculated from plots based on the equation:

$$\ln I = \ln I_0 - kt \qquad \text{(Eq. 6)}$$

where I_0 is the initial concentration of I. Results are given in Tables I and II. Rate constants for loss of I as a function of pH were determined directly from the hydrochloric acid studies and indirectly from the buffer data by extrapolation to zero buffer concentration by the methods described in Table VI. Although the phosphate data showed a linear buffer dependency (7), the pH region 2.8–5.7 was characterized by nonlinear plots for k *versus* buffer as shown in Fig. 4. The buffer system that allowed the most dilution at a given pH was chosen to make the estimates of the intercepts of the curves.

In the alkaline region the absorbance of I in the 250–350-nm. region was found to decrease as a function of time, resulting in an

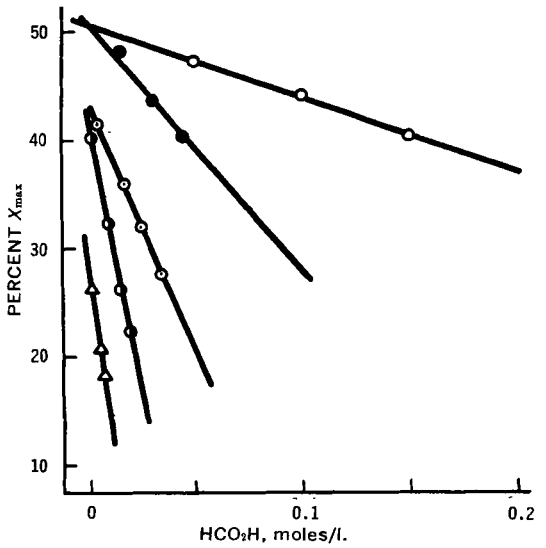

Figure 5—*Maximum yields of the intermediate,* X, *formed during the deamination of arabinosylcytosine in formate buffer as a function of formic acid concentration at 70°. Key: pH 2.8,* ○; *pH 3.2,* ●; *pH 3.6,* ⊙; *pH 3.9,* ◑; *and pH 4.2,* △.

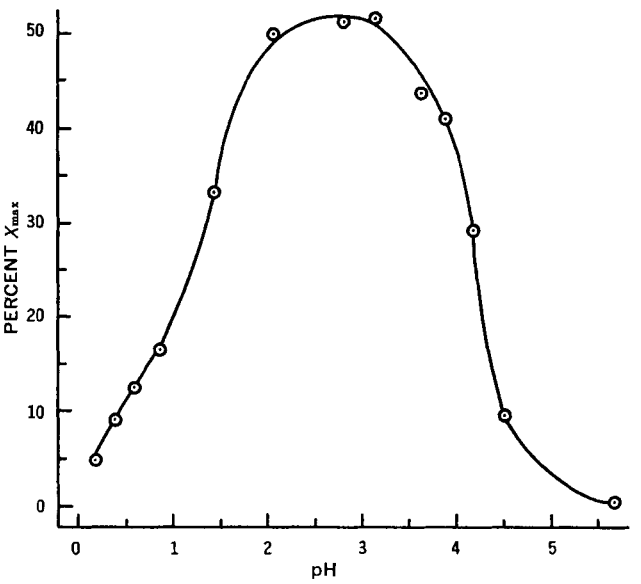

Figure 6—*The pH profile for the maximum yields of the intermediate,* X, *formed during the deamination of arabinosylcytosine at 70°. The yields in pH region 0–2 were obtained directly in hydrochloric acid, and the rest were obtained indirectly by extrapolation of data to zero buffer concentration as illustrated in Fig. 5.*

eventual loss of the UV absorption spectrum. Since the chromophore was completely lost and the final absorbance was zero, the apparent first-order rate constants for loss of I were calculated from the equation:

$$\ln A = \ln A_0 - kt \qquad \text{(Eq. 7)}$$

where A is the absorbance at a given wavelength. Results are given in Table III where A at 290 nm. was employed to obtain the best first-order plots.

The values of E_a and log A were calculated as a function of pH using the Arrhenius equation. These values are employed in the *Discussion* section to predict the stability at room temperature.

Kinetics of Deuterium Exchange and Loss of I in Deuterated Solvents—Pseudo-first-order rate constants for the exchange of D for the H_5 proton were calculated from the slopes of linear plots of $\ln (f - f_\infty)$ *versus* time, where f has been defined in Eq. 3, and Fig. 1 shows a typical change in NMR spectrum obtained during a deuterium-exchange reaction. The value for f_∞ was determined by reiteration to obtain log plots having the longest duration of linearity.

Rate constants for the loss of I in the deuterated solvent systems were determined using Eq. 6 where the assays were performed in triplicate over a period of time that extended well beyond the deuteration studies due to the large difference in the rates of exchange and degradation. Table IV lists the results and allows direct comparison between the exchange rates and the stability of I.

Effect of Reaction Conditions on Intermediate Formation—Plots of the concentration of reaction components as a function of time were constructed by calculating the concentration of I, II, and X using Eqs. 1, 2, and 4. These plots were typical of two consecutive first-order rate processes, where X is a reactive intermediate formed from I during its hydrolytic deamination to II. Plots representing the concentration of X as a function of time passed through a maximum as illustrated in Fig. 2. The maximum yield of % X_{max} defined as:

$$\% X_{max} = 100X_{max}/(I)_0 \qquad \text{(Eq. 8)}$$

was determined as a function of pH, buffer, and temperature. At a constant pH, the largest values of % X_{max} were obtained from the studies with the most dilute buffer concentrations as illustrated in Fig. 5. The % X_{max} values in the absence of buffers were estimated from the intercepts of plots such as those in Fig. 5. These intercept values were used to construct the pH profile for % X_{max} in the absence of buffer shown in Fig. 6. The reaction conditions and the resulting yields are given in Table VII. The data regarding the formation of X were used to produce maximum yields of the intermediate in order to carry out the characterization studies.

UV Absorption Characteristics of Intermediate—Since the assays for I and II were based on the absorption at 260 and 280 nm. in 0.1 *M* HCl, it was necessary to determine what contribution, if any, X made to the absorbance in this spectral region. A reaction mixture containing 50% X was assayed for I and II, and the UV spectrum was determined. This spectrum was compared to that obtained for a simulated mixture of I and II. There was no difference between the two spectra in the 240–320 nm. region, indicating that the intermediate did not interfere with the UV assay for I and II. The UV spectrum for X was also determined in 0.1 *M* Na_2HPO_4. In this case the instability of X made it necessary to use an extrapolation procedure. The spectrum at time zero was obtained by extrapolating first-order plots for the absorbance at each wavelength to time zero. The resulting spectrum was again similar to that for a simulated mixture of I and II, indicating that X did not influence the UV spectra in phosphate solution.

Spectrophotometric Differential Assay for X—I and II are stable in boric acid–borate (0.32 *M* each) buffer at 35° during a 10-min.

Table VII—Percent Yield of Intermediate at Its Maximum Value, % X_{max}, Formed during Deamination of Arabinosylcytosine to Arabinosyluracil

pH	% X_{max}
70°	
0.15	4.7
0.38	8.8
0.56	12.4
0.86	16.2
1.42	33.4
2.08	49.6
2.80	51.0
3.15	51.5
3.63	43.5
3.90	41.0
4.18	29.0
4.49	9.5
5.7–7.8	0.0
80°	
0.16	7.9
0.27	9.4
0.39	10.8
0.56	12.9
0.85	17.1
1.43	32.1
2.08	48.3

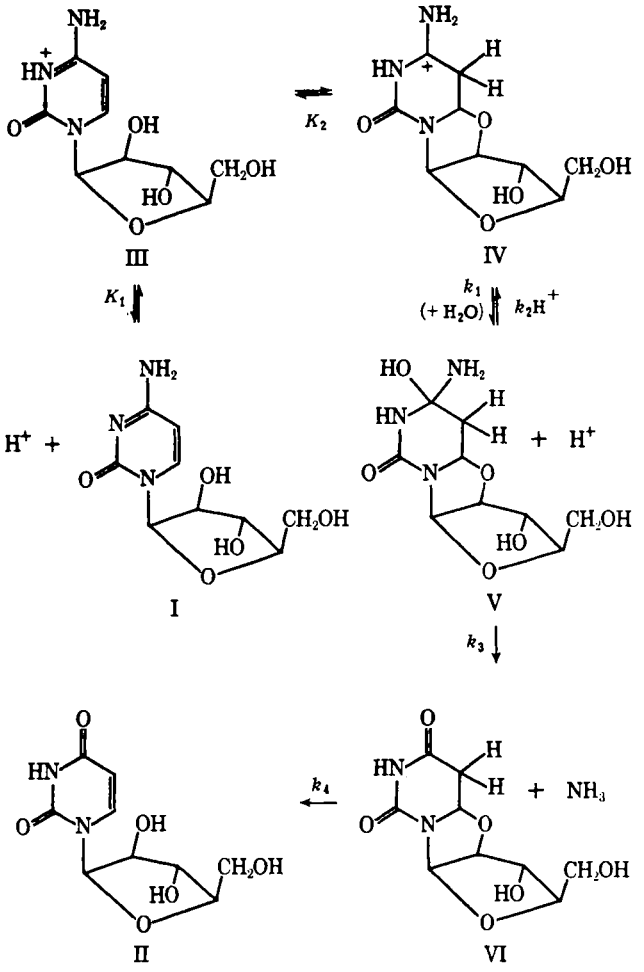

Scheme I

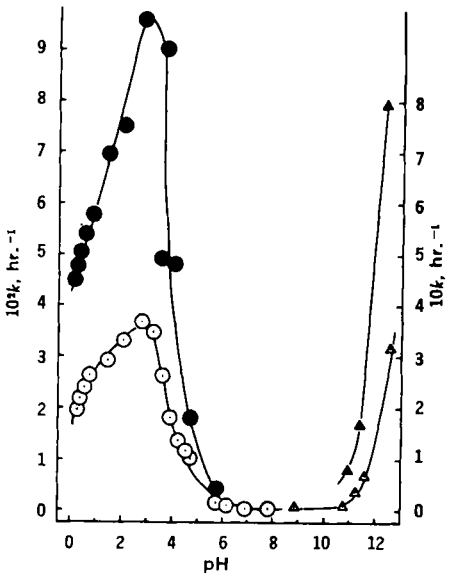

Figure 7—*Observed first-order rate constants for loss of arabinosylcytosine at 70° (○, △) and 80° (●, ▲) as a function of pH. The values for the circles are represented by the scale on the left ordinate (10³ k); the values for the triangles are represented by the scale on the right ordinate (10 k).*

time interval, which is sufficient to convert the intermediate *X* to II. The concentration of *X* can thus be determined by assaying for II, according to Eq. 2, before and after treatment with borate buffer at 35°. Phosphate buffers can also be employed for the conversion, but a longer time interval is required. However, it was found that 0.2 *N* NaOH results in material loss since the sum of the final concentrations of I and II was less than I_0.

TLC Separation of Reaction Components—When the plates were made with a slurry of silica gel GF_{254} in distilled water, the resulting chromatograms showed only two spots visible under UV light. In the benzene–methanol developing system, the R_f values were 0.07 and 0.25, corresponding to I and II, respectively. During the evaporation of the developing solvent from the plate, a third spot, R_f 0.34, slowly became visible by UV detection. Preparation of the slurry in 0.1 *M* HCl instead of distilled water resulted in failure to achieve UV detection of the third spot (R_f 0.34), which became visible under UV light only after spraying the plate with 1 *N* NaOH. The new R_f values were 0.07, 0.17, and 0.27 for I, II, and *X*, respectively. For the water-saturated butanol–propanol developing system and a slurry of silica gel GF_{254} in 0.1 *M* HCl, the R_f values were 0.45, 0.55, and 0.70 for I, *X*, and II, respectively.

Two-dimensional chromatography using water-saturated butanol–propanol (3:1) was used to demonstrate the conversion of *X* to II as follows. Two compounds corresponding to R_f 0.45 and 0.70 were detected after the first separation. On spraying the plate with 1 *N* NaOH, *X* (R_f 0.55) became visible by UV detection. When the plate was developed in a direction perpendicular to the first, the R_f values for I and II remained constant, whereas the R_f value for *X* was the same as that for II, indicating that *X* was converted to II. A similar demonstration was carried out using benzene–methanol (3:1).

Preparative TLC allowed I, *X*, and II to be separated in bands with R_f values of 0.40 (I), 0.49 (*X*), and 0.57 (II). Attempts to isolate and crystallize *X* from the middle band failed due to the instability of *X* which continually formed II during the workup.

Kinetics of Instability of *X*—The rate constants, *k*, for the conversion of *X* to II were determined by plotting ln *X versus* time where the concentration of *X* is defined by Eq. 4. Values for the first-order rate constants, *k* (Table V), were shown to be dependent upon buffer concentration. Catalytic constants were calculated from equations previously published for the phosphate buffer system (8). The values of the catalytic constants are 88.2 l. mole^{-1} hr.$^{-1}$ at 55.5° and 48 l. mole^{-1} hr.$^{-1}$ at 45° for $k_{HPO_4^{-2}}$. The values for $k_{H_2PO^-}$ are negligible.

DISCUSSION

Prediction of Stability in Aqueous Solution—Data from Tables III and VI were employed to construct the plots for *k versus* pH as shown in Fig. 7. It can be seen from this figure that I is most stable in the neutral pH region. The apparent first-order rate constants, *k*, for the deamination of I in 0.06 *M* phosphate buffer, pH 6.9 (47, 55, 60, and 70°), were utilized to calculate E_a (7). An Arrhenius plot of log *k versus* $1/T$, where *T* is the absolute temperature, yields a value for E_a which was determined to be 16.4 kcal. mole^{-1}. Calculation of the rate constant at 25° yields the value 2.2×10^{-5} hr.$^{-1}$. Substitution of the rate constant in Eq. 9 yields the time required for a 10% reduction in potency:

$$t_{0.9} = -\ln 0.9/k \qquad \text{(Eq. 9)}$$

This is calculated to be 6.5 months.

Proposed Mechanisms for Acid-Catalyzed Degradation of Arabinosylcytosine in Aqueous Solution—The pH profile for loss of I in aqueous solutions may be conveniently discussed in two parts. In the acid to neutral region, pH 0–7.8 in Fig. 7, I undergoes deamination to yield II *via* an intermediate, *X*, which is formed in maximum yield at pH 2–3 and is not formed in detectable yields at pH 5.5–7.8 (Fig. 6). The observed rate constant for the loss of I in the absence of buffer catalysis was found to pass through a maximum value at approximately pH 2.8 (Fig. 7).

Scheme I is consistent with the kinetic data reported here. The dissociation constant, K_1, represents the loss of a proton by III to form its conjugate base I. The pKa of III is known and was redetermined spectrophotometrically under the concentrations employed in this study to be 4.2. Attack by the 2′-hydroxyl group to form the 6,2′-cyclic intermediate, IV, was discussed previously (4). Scheme I suggests that IV would achieve equilibrium with III as

described by the constant K_2. Evidence for a rapid equilibrium between IV and III and thus IV and I is given in Table IV, where it can be seen that the deuteration of I occurs 60–100 times faster than deamination in deuterium oxide. Thus the concentration of IV would be dependent upon that of III, which is pH dependent since it involves protonation of I. However, IV must be regarded as a reactive intermediate which does not exist in measureable concentrations. This supposition is supported by the fact that the UV absorptivity of I in 0.1 *M* HCl is not less than that of cytidine.

Scheme I predicts that the loss of I would pass through a maximum at some pH less than the pKa of III, which is 4.2. The following derivation illustrates this point. The concentration of substrate as determined by the assay using Eq. 1 would be:

$$C = (\mathrm{I}) + (\mathrm{III}) + (\mathrm{IV}) \qquad \text{(Eq. 10)}$$

and:

$$dV/dt = k_1(\mathrm{IV}) - k_2\mathrm{H}^+(\mathrm{V}) - k_3(\mathrm{V}) \qquad \text{(Eq. 11)}$$

Applying the steady-state assumption to V yields:

$$(\mathrm{V}) = k_1(\mathrm{IV})/(k_3 + k_2\mathrm{H}^+) \qquad \text{(Eq. 12)}$$

since:

$$K_1 = (\mathrm{I})\mathrm{H}^+/\mathrm{III} \qquad \text{(Eq. 13)}$$

and:

$$K_2 = (\mathrm{III})/(\mathrm{IV}) \qquad \text{(Eq. 14)}$$

then:

$$C = (\mathrm{IV})(1 + K_2 + K_1K_2/\mathrm{H}^+) \qquad \text{(Eq. 15)}$$

Substitution for V in Eq. 11 using Eq. 12 gives:

$$-dC/dt = k_1(\mathrm{IV}) - k_2\mathrm{H}^+k_1(\mathrm{IV})/(k_3 + k_2\mathrm{H}^+) \qquad \text{(Eq. 16)}$$

which may be written in terms of C using Eq. 15:

$$-dC/dt = [k_1k_3\mathrm{H}^+/(k_2\mathrm{H}^+ + k_3)(\mathrm{H}^+ + K_2\mathrm{H}^+ + K_1K_2)]C \qquad \text{(Eq. 17)}$$

It can easily be shown that the observed first-order rate constant for loss of I, k_{obs}, will have the general shape illustrated in Fig. 7 when plotted as a function of pH. From Eq. 17, it is apparent that:

$$k_{obs} = k_1k_3\mathrm{H}^+/(k_2\mathrm{H}^+ + k_3)\,(\mathrm{H}^+ + K_2\mathrm{H}^+ + K_1K_2) \qquad \text{(Eq. 18)}$$

When $\mathrm{pH} < \mathrm{pK}_1 - 2$, then:

$$k_{obs} = k_1k_3/(k_2\mathrm{H}^+ + k_3)(1 + K_2) \qquad \text{(Eq. 19)}$$

and since $K_2 \gg 1$, then:

$$k_{obs} = k_1/(K_2 + k_2K_2\mathrm{H}^+/k_3) \qquad \text{(Eq. 20)}$$

and:

$$1/k_{obs} = K_2/k_1 + k_2K_2\mathrm{H}^+/k_1k_3 \qquad \text{(Eq. 21)}$$

Equation 21 predicts that a plot of $1/k_{obs}$ *versus* H^+ would be linear with slope k_2K_2/k_1k_3 and intercept K_2/k_1. Equation 21 shows good agreement with Fig. 8 at 70°, where the least-squares regression lines have regression coefficients of 99.93 and 99.96% (excluding the one experimental point not on the line in each case). Thus, Eq. 20 predicts a decrease in the observed rate constant as pH is decreased in the acid pH region which agrees with that illustrated in Fig. 7. That figure also shows a decrease in k_{obs} with increasing pH in the pH region higher than the pKa. Therefore, if $\mathrm{pH} > \mathrm{pK}_1 + 2$, Eq. 18 becomes:

$$k_{obs} = k_1\mathrm{H}^+/(K_1K_2 + K_1K_2k_2\mathrm{H}^+/k_3) \qquad \text{(Eq. 22)}$$

which can be rearranged to give:

$$1/k_{obs} = K_1K_2/k_1\mathrm{H}^+ + K_1K_2k_2/k_1k_3 \qquad \text{(Eq. 23)}$$

which predicts a linear plot of $1/k_{obs}$ *versus* $1/\mathrm{H}^+$ with positive slope

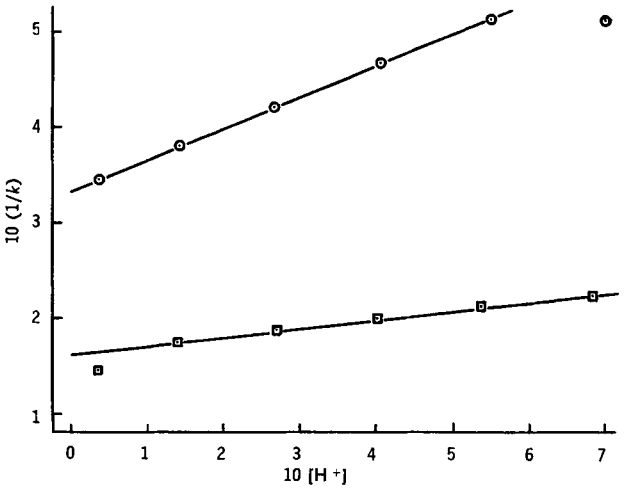

Figure 8—*Least-squares regression lines for plots of reciprocal values of observed first-order rate constants for arabinosylcytosine loss* versus *the hydrogen-ion activity,* $[H^+]$, *at 70°* (⊡) *and 80°* (⊙). *The two points that do not lie on the lines were omitted from the regression calculations.*

of K_1K_2/k_1. Thus, k_{obs} *versus* pH would decrease with increasing pH in the pH region above the pKa, in agreement with Fig. 7.

Scheme I and its corresponding equations would indicate VI as a possible intermediate in degradation of I to II. The various characteristics of the unknown intermediate, previously called *X*, can be easily ascribed to VI. For example, VI would not be expected to have a UV absorption spectra of any significance in the 240–320-nm. region. The decyclization of VI would be expected to resemble the mechanism for the dehydration of an aldol. Dehydration of the aldol, streptovitacin A, has been reported to be 10^5 times faster in base than in acid (8). Compound VI would therefore be expected to show greater stability in acid than in base in agreement with the observed stability of *X*, which is extremely unstable in base relative to acid and subject to general-base catalysis but not general-acid catalysis in phosphate buffers at 45–55°, pH 5.5–7.6. Thus, VI would be expected to yield II readily in the presence of base and also to yield II, albeit less readily, in the presence of acid, but VI would not be expected to give rise to I. This is in agreement with the observed properties for the intermediate *X*.

Proposed Mechanism for Arabinosylcytosine Degradation in Alkaline Solution—The loss of I in solutions of alkaline pH is not accompanied by a concomitant increase in II. Instead, the degradation of I in alkali is characterized by a complete loss of UV spectra. This suggests that the pyrimidine ring is being hydrolyzed, as was shown in several previous reports for uracil nucleosides. Fox *et al.* (9) showed that the UV absorption spectrum of 1β-D-arabinofuranosyl-5-fluorouracil is completely lost within 30 min. at 60–70° in the presence of 0.1 *N* NaOH due to formation of the open-chain ureide, VII, which was isolated in nearly quantitative yield.

When 1β-D-arabinofuranosyl-5-fluorocytosine was heated in 0.1 *N* NaOH at 60–70° for 30 min., its UV spectrum was also completely lost but the yield of VII was approximately 50%, indicating the loss of substrate to other nonchromophoric product(s) in addition to VII. Fox *et al.* (9) also reported that I and II undergo much slower loss of absorption under the above conditions, thus indicating that the fluorine atom on C-5 enhances the suscepti-

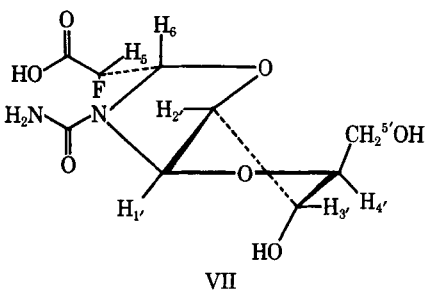

VII

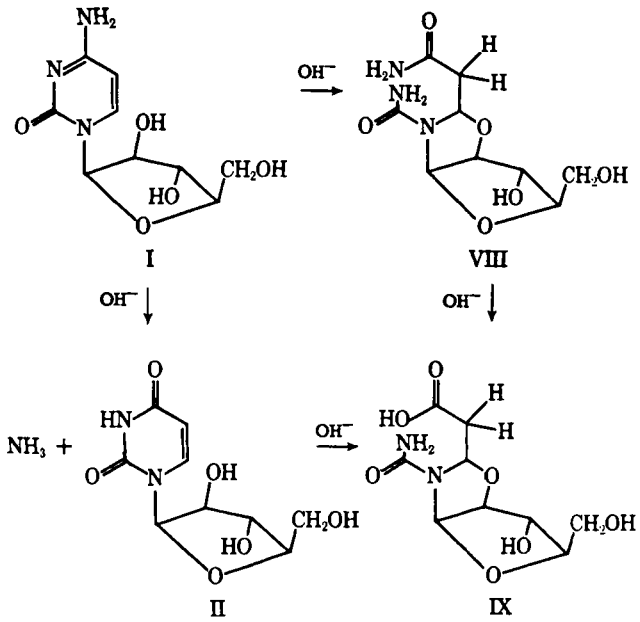

Scheme II

bility of C-6 to nucleophilic attack. A detailed mechanism for the formation of VII due to intramolecular attack by the 2′-hydroxyl anion in alkaline solutions to form the 6,2′-anhydronucleoside and a lucid discussion of the reaction may be found in that reference and will not be repeated here.

Although the products of the reactions of I and II in 0.1 *N* NaOH at 60–70° were not investigated by Fox *et al.* (9), they suggested that 6,2′-anhydro formation in alkali is probably a general characteristic of those pyrimidine ring nucleosides that have a 2′-hydroxyl in the *cis*-position relative to the ring. Loss of I in the present study at pH values of 9–13, 70–80°, would be expected to undergo reactions similar to 5-fluoro derivatives at slower rates. Scheme II illustrates the probable reaction pathways for loss of I in alkali based on the work of Fox *et al.* (9) and the kinetic studies reported here.

It is interesting to contrast 6,2′-anhydro formation under acidic conditions ultimately leading to II (Scheme I) with intramolecular attack in alkali which yields VIII and/or IX. Attack of the 6-position by the 2′-hydroxyl in acid is made possible by the protonation of N-3 with resultant electron deficiency at C-6 (4, 7). In alkali, 6,2′-anhydro formation is attributed to attack by the 2′-oxygen as an anion (9). Perhaps more significant is the difference between proposed intermediates for the two routes. Fox *et al.* (9) suggested XI as the precursor to VII. This compound is the 5-fluoro derivative of the conjugate base of VI. It would thus appear that the protonated form of the 6,2′-anhydro intermediate, VI, yields the corresponding uracil derivative, II, whereas its conjugate base would be expected to yield the ureide structure, IX (which is VII with a 5-H in place of 5-F). This is consistent with the observation that the

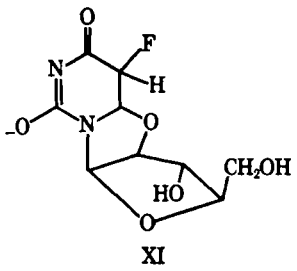

XI

intermediate *X* was readily converted to II at pH values 5–9, 35–55°, whereas degradation of II in 0.2 *N* NaOH resulted in loss of material to nonchromophoric products. (See the section entitled *Spectrophotometric Differential Assay for* X, Table V, and Fig. 3.) Since a pKa of 9–10 represents a reasonable estimate for VI, it is conceivable that the degradation product is kinetically controlled and that the acid, VI, undergoes a reaction analogous to aldol dehydration to yield II whereas its conjugate base undergoes pyrimidine ring hydrolysis to yield the ureide structure similar to VII.

REFERENCES

(1) W. Bergmann and R. J. Feeney, *J. Org. Chem.*, **16,** 981 (1951).

(2) R. W. Carey and R. R. Ellison, *Clin. Res.*, **13,** 337(1965).

(3) J. P. Howard, N. Cevik, and M. L. Murphy, *Cancer Chemother. Rep.*, **50,** 287(1966).

(4) R. E. Notari, M. Lue Chin, and A. Cardoni, *J. Pharm. Sci.*, **59,** 28(1970).

(5) D. V. Santi, C. F. Brewer, and D. Farber, *J. Heterocycl. Chem.*, **7,** 903(1970).

(6) P. G. Glascoe and F. A. Long, *J. Phys. Chem.*, **64,** 188(1960).

(7) R. E. Notari, *J. Pharm. Sci.*, **56,** 804(1967).

(8) R. E. Notari and S. M. Caiola, *ibid.*, **58,** 1203(1969).

(9) J. J. Fox, N. C. Miller, and R. J. Cushley, *Tetrahedron Lett.*, **1966,** 4927.

(10) G. Åkerlöf and G. Kegeles, *J. Amer. Chem. Soc.*, **62,** 620 (1940).

(11) H. S. Harned and B. B. Owen, "The Physical Chemistry of Electrolyte Solutions," 3rd ed., Reinhold, New York, N. Y., 1958.

ACKNOWLEDGMENTS AND ADDRESSES

Received January 4, 1972, from the *College of Pharmacy, Ohio State University, Columbus, OH 43210*

Accepted for publication April 19, 1972.

Supported in part by funds from the American Cancer Society Institutional Grant IN-16K, RF 2786-J.

• National Science Foundation Undergraduate Research Participant, 1970–1971.

▲ To whom inquiries should be directed.